

High-Amplitude Time Reversal Focusing of Ultrasound in Air

Carla Butts Wallace

A thesis submitted to the faculty of

Brigham Young University

In partial fulfillment of the requirements for the degree of

Bachelor of Science

Brian E. Anderson, Advisor

Department of Physics and Astronomy

Brigham Young University

August 2020

Copyright © 2020 Carla Wallace

All Rights Reserved

ABSTRACT

High-Amplitude Time Reversal Focusing of Ultrasound in Air

Carla Butts Wallace

Department of Physics and Astronomy

Bachelor of Science

Time reversal (TR) focusing of airborne ultrasound in a room is demonstrated. Various methods are employed to increase the amplitude of the focus. These methods include creating a small wooden box (or chamber) to act as a miniature reverberation chamber, using multiple sources, and using the clipping processing method. The use of a beam blocker to make the sources more omnidirectional is examined, and it is found that for most source/microphone orientations, the use of a beam blocker increases the amplitude of the focus. A high-amplitude focus of 134 dB peak re 20 μ Pa SPL is generated using TR. The waveform and spectrum of the focus are examined to determine if the focus is loud enough to generate nonlinear effects in the air. Using 4 sources centered at 36.1 kHz and another 4 sources centered at 39.5 kHz, nonlinear difference frequency content near 3.4 kHz is observed in the focus signal. If the nonlinearities are generated in the air, the TR setup could perhaps be used to create a virtual sound source (spherically symmetric parametric array) within a room, from which audible sound may propagate.

Keywords: Time Reversal, Parametric Array, Beam Blocker, Ultrasound, Focusing, Ultrasonic Jamming, Private Communication

Acknowledgments

I would like to thank the college of Physical and Mathematical Sciences at BYU for funding this research and allowing me to work as a research assistant.

I would like to thank my advisor, Dr. Anderson, for his mentorship. I am grateful for the time he invests in mentoring undergraduate students such as myself. I would also like to thank Dr. Traci Neilsen for her training and mentorship when I first joined the acoustics research group at BYU.

I would like to thank John Ellsworth for designing and building the transformers we used with our piezoelectric sources. I would also like to thank Adam for his work on the software we used to run the TR experiments. I would also like to thank Jeremy and everyone in the machine shop for helping us create our apparatus.

I would like to thank my parents for fostering a love of science, and for their support and encouragement throughout my schooling. Lastly, I would like to thank my husband for his support and encouragement. He has always encouraged me to grow academically and shoot for my dreams.

Table of Contents

Table of Contents	vi
List of Figures.....	vii
Chapter 1 Introduction	1
Chapter 2 Setup.....	8
2.1 Equipment and Software	8
2.2 Signal Processing.....	9
2.3 Miniature Reverberation Chamber.....	10
2.4 Source Directivity	13
2.5 Transducer Response.....	16
2.6 Time-Varying Impulse Responses	23
Chapter 3 Results	25
3.1 Effect of Directivity on TR Focal Amplitudes	25
3.2 Peak Levels Achieved at Focus.....	27
3.3 Nonlinear Difference Frequency Generation	28
Chapter 4 Conclusions	30

List of Figures

Fig. 1. Photograph of the 0.58 m ² box used for the time reversal experiments.....	11
Fig. 2. Setup diagram for the absorption coefficient measurement inside an anechoic chamber.....	12
Fig. 3. Photograph and beam patterns of the ultrasonic source. a) Photograph of the source inside the 3D-printed holder, with a beam blocker. b) and c) Beam patterns with and without blockers (dB relative to the no blocker case at 0°) for b) 35.1 kHz - 37.1 kHz bandwidth and c) 38.5 kHz - 40.5 kHz bandwidth, respectively.....	15
Fig. 4 (a) Average electrical impedance of 8 piezoelectric sources. (b) Average acoustic frequency response of 8 piezoelectric sources at 0° relative to microphone.	17
Fig. 5. Setup diagram using generator card, amplifier (triangle), DC blocking capacitor, 4:1 transformer, and source.....	18
Fig. 6. a) Peak focal amplitude versus forward-step bandwidth with 4 sources centered on 36.1 kHz and 4 sources centered on 39.5 kHz. b) Maximum in difference frequency band vs. forward-step bandwidth. c) Energy in difference frequency band vs. forward-step bandwidth...	20
Fig. 7. (a) Configuration of 2 microphones end-to-end, with gridcaps touching. (b) Amplitudes recorded by 2 microphones, 28 cm away from a PAL. Input voltage from the generator card to the PAL is varied. (c) Amplitudes recorded by 2 microphones, 211.5 cm away from PAL. Input voltage from generator card to PAL is varied. 1 kHz signals from both mics lie almost exactly in the same place.....	22
Fig. 8. Time reversal peak focal amplitude for various angles of eight sources with respect to the microphone with and without blockers in place. Forward step chirp bandwidths are (a) 35.1 – 37.1 kHz and (b) 38.5 – 40.5 kHz.....	26

Fig. 9 (a) Scaled spectra of focus signal. (b) Scaled focus signal spectra zoomed in on difference frequency content. (c) Difference frequency energy (3-4 kHz) vs. primary frequency energy (35-40 kHz). (d) Maximum within difference frequency band vs. maximum within primary band. 29

Chapter 1 Introduction

Time-reversal (TR) signal processing is a technique which can be used to focus acoustic wave energy to a point in space.^{1,2} The method employs multiple sources and/or multiples reflections off walls in a room, which are timed in such a way that the sound waves add constructively at a focal point within the room. During the so called forward step of TR, if an impulsive acoustic signal is broadcast from point A in a room and recorded with a microphone at point B, the signal that is recorded with the microphone is the impulse response between point A and point B. The waveform of this impulse response consists of the direct arrival, followed by multiple reflections. If this waveform is reversed in time, and broadcast from point A, (the so called backward step of TR) the later reflections will be broadcast first, allowing them time to travel the longer paths to point B. Then the early reflections are broadcast, and finally the direct arrival is broadcast. All of the emissions from the time-reversed impulse response (TRIR) arrive at point B at the same time and constructively interfere to create a TR focus of sound. The

waveform that arrives at point B is a band-limited approximation of the impulse originally broadcast from point A. In truth, the emissions from the time-reversed impulse response (TRIR) will travel many additional paths and arrive at point A at various times creating artifacts in the waveform before and after the time of focus, called side lobes³, but there is a time at which these impulsive parts of the TRIR all arrive at point B simultaneously. Thus, energy may be focused from one or more remotely placed sources to a selected location within a room.

In the experiments conducted for this thesis, rather than sending an impulse from point A, the impulse response is obtained by broadcasting a chirp signal from point A, recording the chirp response at point B, and calculating the band-limited impulse response through a cross correlation of the chirp response with the input chirp signal.^{4, 5}

The first application of TR was signal transmission in the ocean.^{6, 7} Candy *et al.*^{8,9} and Meyer *et al.*¹⁰ applied TR to communication in a reverberant room, using audible sound in air.⁸⁻¹⁰ Ribay *et al.* did numerical simulations and asserted that TR focal amplitude is proportional to the reverberation time of the room.¹¹ Denison and Anderson validate this relationship in the case that reverberation time changes due to a changing absorption coefficient, but they show numerically and experimentally that when reverberation time is a function of room size, a smaller room (with a shorter reverberation time) yields a higher focal amplitude.¹² Willardson *et al.* created a high-amplitude focus of audible sound in air, where the peak pressure amplitude at the focus was 173.1 dB peak re 20 μ Pa. At these pressure levels, they observed nonlinear effects from the air including high frequency sound generation and waveform steepening.¹³

Applications of high-amplitude TR using ultrasound include non-destructive evaluation (checking for cracks in materials),¹⁴⁻¹⁸ lithotripsy for destroying kidney stones,^{19, 20} and treatment

of brain tumors.^{21, 22} In all of these applications, ultrasound is used in a solid or in the human body. Montaldo *et al.* used TR in a solid waveguide to create a high-amplitude focus of ultrasound, with an intended application to lithotripsy of kidney stones.¹⁹ They use one-bit TR, which also increases the amplitude of the focus. They achieved amplitudes that were 15 times greater than a standard technique. They asserted that amplification is proportional to the bandwidth of the transducer. Young *et al.* studied the effect of impulse response modification techniques, in order to increase focal amplitude, with an application to non-destructive crack detection.²³

TR has been used with ultrasound in water, solids, and in the human body. TR has also been used with audible sound in air. However, to the best of our knowledge, TR has not been used with ultrasound in air. This thesis demonstrates the use of TR with ultrasound in air. Potential applications of remotely-focused, airborne ultrasound include selective microphone jamming, private communication, targeted pest deterrents, non-lethal weapons, and the creation of a “virtual” loudspeaker.

It has been shown that high-amplitude ultrasound can be used to create intermodulation distortion in a microphone (due to nonlinearities in the diaphragm and/or amplifier), which causes it to record pseudo signals, effectively masking other audible signals that the microphone records.^{24, 25} This is known as “ultrasonic jamming.” TR could be used to selectively jam a target microphone.

Ultrasonic TR could also be used to send targeted inaudible signals. Since ultrasound is outside the range of human hearing, ultrasound can be used for inaudible data transfer without using electromagnetic waves. As Roy *et al.* show, ultrasonic frequencies can be used to transfer

data, which is demodulated and recorded by an ordinary microphone (such as those found in cell phones).²⁴ They explore the potential of ultrasound used in this way to transfer data. TR could be used in a similar way to send an inaudible acoustic communication that is recorded by the microphone, but TR adds the capability of targeting a specific microphone.

Sending targeted inaudible signals could also be used as a pest deterrent. For instance, if a pest emits an ultrasonic signal, the recording can be time reversed and played back from an ultrasonic emitter at the location of the microphone. Thus, a time-reversed version of the original pest's signal will be focused back at them. Ultrasound is already used in many pest-deterrent devices, but the ability to target the pests could allow the use of lower-amplitude ultrasound in the surrounding environment. One pest deterrent was measured by Ueda *et al.* to have a sound pressure level (SPL) of around 130 dB right under the device²⁶. The effects of high-amplitude ultrasound on humans are starting to be studied²⁷⁻²⁹ and it may be advantageous to avoid exposing humans to high-amplitude ultrasound that may be present near traditional ultrasonic pest deterrents.^{26, 30, 31}

High-amplitude ultrasound has been reported to produce undesirable effects in humans, including symptoms such as headaches.^{27, 31} If the impulse response between ultrasonic source and victim is known, TR could possibly be used to create targeted non-lethal weapons.

If high enough amplitudes are achieved in TR focusing, it might create a difference frequency due to nonlinearities in the air itself. In such a case, it may be possible to create a spherically symmetric parametric array, which generates audible sound that propagates away from the focus location (by using two focused, primary ultrasonic signals at two different frequencies to generate a difference frequency). The idea of combining the parametric array with

other ultrasonic applications, including TR, is mentioned briefly by Shi *et al.*,³² but the implementation is not explored. Using two different frequencies to create a high-amplitude TR focus may create a “virtual” loudspeaker in the sense that audible sound seems to come from a location where no hardware is present. This would enable the creation of virtual sound sources within rooms, in locations where it may be difficult to place a traditional loudspeaker. Elaboration on the parametric acoustic array and its potential connection to a difference frequency generated by TR is included in the following paragraphs.

A parametric array is created due to the nonlinearities of air when high-amplitude sound at two different primary frequencies (f_1 and f_2) propagate in the same direction (collinearly). The nonlinear terms produce sum and difference frequencies. The difference frequency, $|f_1 - f_2|$, is of particular interest because this frequency can be audible while the primary frequencies are above the range of human hearing. There are commercially available parametric array loudspeakers that use two or more ultrasonic frequencies to generate an audible difference frequency. The difference frequency is highly directional because it's generated by the nonlinear mixing of ultrasonic frequencies as they propagate, forming a virtual end-fire array in the air.³³ The difference frequency initially becomes louder as the primaries propagate together until the point where the amplitudes of the primaries have significantly decreased due to atmospheric absorption and spherical spreading.³⁴ The audible difference frequency is independent from the primary frequencies in the sense that it continues to exist even after the primaries have died out.³⁵ The difference frequency beam inherits the directivity of the primary frequencies.

In order to be categorized as a parametric array, the two primary frequencies must travel in the same direction (i.e. be collinear.) Note: the terms “collinear” and “collimated” refer to separate concepts within this thesis. “Collinear” means that the two primary frequencies travel in the

same direction as each other. “Collimated” means that a single sound beam has no geometric spreading.) There is much debate in the literature concerning the theory on noncollinear interaction of sound with sound.³⁵⁻⁴⁵ While it seems undisputed that a difference frequency can exist within the interaction region of two primaries,^{40, 45} it is contested whether it is possible for the difference frequency to propagate away from the interaction region of noncollinear primary beams.³⁵⁻⁴⁵ Hamilton specifically mentions that local interaction of sound with sound, where the difference frequency does not necessarily propagate away from the region of interaction, may happen at the focus of converging waves.⁴⁵ Therefore, because TR creates a focus of converging waves, the presence of these (local) noncollinear interactions may need to be considered as a possible source of the difference frequencies observed in this study. Since difference frequencies produced in the interaction region of noncollinear waves likely do not propagate away from the region of interaction, we cannot assume that all of the difference-frequency energy recorded at the focus propagates away from the focal region (even if we rule out microphone distortion).

During time reversal focusing, waves converges toward the focus location with spherical symmetry, constructive interference occurs, and then waves diverge with spherical symmetry.⁴⁶ Since the waves converge toward and then diverge away from the focal location, one can argue that there could be a fair degree of shared propagation paths for two focused primaries using TR. Thus, it seems that an outward propagating difference frequency can be created as long as primaries propagate with the same symmetry (they travel in the same direction as each other). They need not be collimated. Because the term “collinear” refers to one Cartesian direction, and we will consider spherically converging and diverging waves, in this thesis we will use the phrase “shared propagation paths” in place of “collinear” to describe two primaries that travel in the same direction. If the environment in which TR is performed is not very reverberant, there

may be only a couple of reflections which propagate toward the focus, and they from disparate directions. Thus, the two primaries might never travel in the same direction as each other, and the difference frequency generation may be limited to a local interaction in the focal region. If we detect a difference frequency at the microphone, we must be aware of the potential of these local effects, which we cannot assume propagate away from the focus.

The purpose of this thesis is to explore methods of optimizing a TR focus of airborne ultrasound in a room. Various methods are explored to increase the amplitude of the TR focus. The use of beam blockers is explored to create more omnidirectional sources. Then a comparison of omnidirectional sources (with the beam blockers in place) to directional sources (without the beam blockers) is made in relation to peak focal amplitude. It is then shown that TR can be used to generate a difference frequency at the focus (the exact source of nonlinearity that generates these difference frequencies has yet to be determined). This thesis acts as a baseline for exploring any of the airborne ultrasonic TR applications mentioned in the above paragraphs.

Chapter 2 of this thesis explains the experimental setup. This includes the use of a wooden box chamber, modifying the directivity of sources (using a beam blocker), equipment used, selection of frequencies used, design of transformers to use with our amplifiers, an evaluation of distortion in the microphones used, and signal processing methods used. Chapter 3 presents experimental results. This includes the dependence of TR focal amplitude on the angle of the source(s) relative to the microphone, comparing both the blocker and no blocker cases. Also included is the maximum focal amplitude achieved with 8 sources. A difference frequency is observed when using 4 sources at one frequency band, and 4 sources at another band. Chapter 4 discusses conclusions.

Chapter 2 Setup

2.1 Equipment and Software

To perform the TR experiments in this thesis, custom LabVIEW software was used that interfaces with the signal generator and digitization cards. The software synchronizes the generation of 8 arbitrary-waveform signals and the digitization of 4 input signals. The software also defines a chirp signal (with optional leading and trailing zeros) to use in the forward step, calculates the impulse response from the recorded sensor response signal, applies optional signal processing techniques (such as one-bit TR) to the time reversed impulse response (TRIR), and saves the recorded signals. This software can also apply a second order zero-phase Butterworth filter to either of the recorded signals (signal response or focus signal), with values for the 3 dB

cutoff frequencies specified by the user. The software allows time-domain averaging of the forward and/or backward signals. The software always uses the same sampling frequency for both the generator and digitizer cards.

Two, four-channel, Spectrum M2i.6022 generator cards (14 bit resolution) and one, four-channel, Spectrum M2i.4931 digitizer card (16 bit resolution) were used for all measurements described here, except for the electrical impedance measurements. Two types of microphones were used: a 6.35 mm (1/4 inch) GRAS 40BE Free-Field Microphone with a 26CB preamplifier, and a 12.7 mm (1/2 inch) GRAS 46AQ Random Incidence Microphone Set. The 6.35 mm microphone is used for all measurements unless specified otherwise. The microphones were used with a G.R.A.S. 12AX 4 Channel CCP Power Module. The ultrasonic sources used here are piezoelectric, Parsonics PAR4012A sources, meant to be driven with frequencies near 40 kHz. For some measurements, the signal from the generator cards were amplified with Tegam 2350 Power Amplifiers (with 50 times gain), used in conjunction with direct-current (DC) blocking capacitors and 4:1 transformers (more details given later). Some measurements did not use any amplification of the source signals.

2.2 Signal Processing

Willardson *et al.* compared 5 signal processing methods that can be applied to a TRIR for audible sound in a room, namely traditional TR, clipping TR, one-bit TR, deconvolution TR, and decay compensation TR.¹³ Of these five methods, they found that clipping yielded the highest-amplitude TR focus. Young *et al.* performed a similar analysis using ultrasonic, elastic waves, yielding similar findings.²³ Based on these results, we chose to apply clipping to our TRIR,

because we were trying to create the highest-amplitude TR focus possible, so that we could have the best chance of observing nonlinear sound propagation in the air during TR focusing. However, methods such as one-bit TR and clipping TR introduce distortion due to the signal processing.²³ This is necessary to consider if we want to look at harmonics generated, but the distortions due to clipping will not produce a difference frequency. Therefore, if a difference frequency is seen in our signal, it came from a source of nonlinearity other than clipping.

2.3 Miniature Reverberation Chamber

A small wooden box with a volume of 0.58 m³ (inside dimensions 83 cm × 105 cm × 66 cm) was created to use as a miniature reverb chamber (see Fig. 1). The dimensions of the box were chosen to correspond to the golden ratio, $2^{1/3} : 4^{1/3} : 1$, therefore the room aspect ratio is identical to the simulations of Denison *et al.*¹² The use of a small box was motivated by their work, where they found that smaller room size increases TR amplitudes with traditional TR (they did not study the effect of room size on TR amplitude with clipping TR). Since atmospheric absorption is a bigger factor at higher frequencies, this was another reason to decrease the size of the box. The box was made of 1.9 cm ($\frac{3}{4}$ inch) medium density fiberboard (MDF). To increase the focal amplitudes further, it might help to make the box more reverberant by painting the inside.

In a subsequent study Denison *et al.* stated that for a TR process in a rectangular room, placing the sources and receivers in the same Cartesian plane increases focal amplitude.⁴⁷ Throughout the TR measurements reported here, the sources and receivers were placed at the same height in the wooden box.



Fig. 1. Photograph of the 0.58 m² box used for the time reversal experiments.

Denison *et al.* showed that TR focal amplitude increases somewhat as distance between source and microphone increases beyond the critical distance for the room.⁴⁷ The critical distance is defined as

$$r_c = \sqrt{\frac{\gamma R}{16\pi}}, \quad (1)$$

where γ is the directivity factor of the sound source (assumed to be 1 in this case, even though the source is not perfectly omnidirectional), and R is the room constant. R is defined as

$$R = \frac{\langle \alpha \rangle_S S}{1 - \langle \alpha \rangle_S}, \quad (2)$$

where $\langle \alpha \rangle_S$ is the average absorption coefficient of the surfaces in the room and S is the surface area of the room.

To find an approximate absorption coefficient for MDF at 40 kHz, a piece of 1.9 cm (¾ inch) MDF board was tested in a small anechoic chamber, which has been shown to be anechoic

in the ultrasound frequency range used here.⁴⁸ The basic setup is diagrammed in Fig. 2. The board was propped up nearly vertically against one wall of the chamber, and a 40 kHz source was placed 82 cm away from the board. The 6.35 mm microphone was placed between the board and the source, 43 cm away from the board and 39 cm away from the source. This allowed enough time for the direct signal to end before the reflected signal could travel to the microphone. The excitation signal was a 2 ms long sine wave pulse at 40 kHz. The recording was sampled at 5 MHz. The measurement was averaged 10 times and high-pass filtered to reduce low-frequency noise. Spherical spreading was observed to begin at about 30 cm from the source. A 1.24 ms segment of both the direct signal and reflected signal was extracted from the waveform, and the root mean square (RMS) amplitudes were compared. These RMS amplitudes of the direct and reflected signals were corrected for spherical spreading before being compared to determine the absorption coefficient, α . At 40 kHz, α of 1.9 cm MDF was found to be $\alpha = 0.115$.

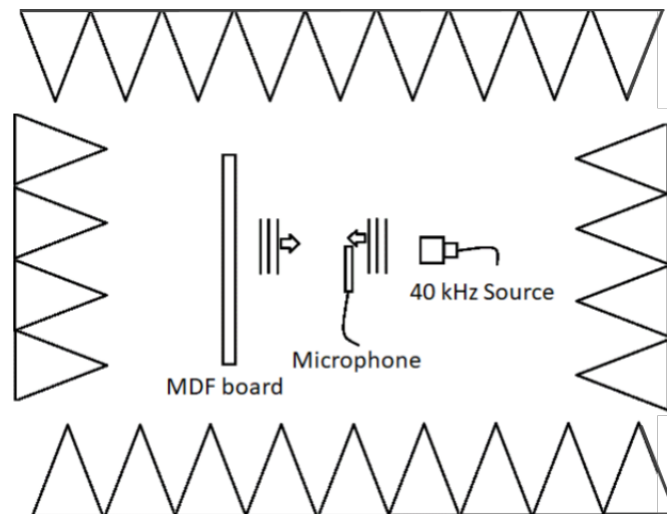


Fig. 2. Setup diagram for the absorption coefficient measurement inside an anechoic chamber.

From this, $r_c = 10.5$ cm in the wooden box chamber at 40 kHz. Throughout the TR experiments in the wooden chamber, the sources were placed at least 11 cm away from the microphone used for TR focusing so that they would always be at least r_c distance away from the microphone.

2.4 Source Directivity

Because the wavelengths used (8.6 mm at 40 kHz) are small relative to the face of the transducers (radius, $a \approx 7$ cm) the waves do not diffract around the transducer ($ka = 22$, where k is the acoustic wavenumber). This means the sources are highly directional, which may not be desirable for high amplitude TR focusing. Because TR relies on multiple reflective paths to create a focus, it is likely advantageous to make the sources more omnidirectional. Incidentally, we tried the method suggested by Anderson *et al.*⁵ to point the directional sources away from the focal location but because the sources are so highly directional, this method proved detrimental to achieving a maximal TR focus amplitude when using the sources without beam blockers. To make the sources more omnidirectional, an aluminum disk with a small hole in the center (outside diameter: 10.2 cm, inside diameter: 8.1 mm, thickness 3.05 mm) was placed in front of each source to act as a beam blocker to scatter the radiation. These disks were held in place with 3D-printed, plastic holders designed to hold the disk $4.8 \text{ mm} \pm 1 \text{ mm}$ away from the face of the source transducer.

To choose the size of the blocker, measurements using a few different blocker sizes were performed. The outer diameter of the blocker and inner diameter of the blocker hole were explored briefly. Three different inner diameters of 12 mm, 8 mm, and 4 mm were achieved by

taping washers of different sizes to the blocker disk (the 12 mm hole had no added washer). A 10 cm outer diameter was used in all these different washer cases. Three different outer diameters were then tested: 6 cm, 10 cm, and 13 cm (with the 8 mm washer in place to keep the inner diameter the same). For each change, a directivity measurement of the source/blocker configuration was taken, and the 40 kHz beam patterns were visually compared. All beam patterns were kept at the same reference distance, so that both the directionality and relative strength of the source could be compared for each configuration. Based on this visual comparison, it was decided to use a beam blocker with an outer diameter of 10 cm and an inner diameter of 8 mm. The frequency response of the sources was measured with the blockers in place, and it was found that the blockers introduce acoustic resonances. Seven standoff distances were tested, and 4.8 cm was selected, because the frequency response had two resonances which were fairly high-amplitude, fairly equal to each other in amplitude, and within the acceptable frequency range (below 41 kHz to avoid the very low impedance frequency range of the sources). Figure 3 shows the effect of the beam blocker on directivity for the two bandwidths (35.1-37.1 kHz and 38.5-40.5 kHz) chosen for the TR experiments.

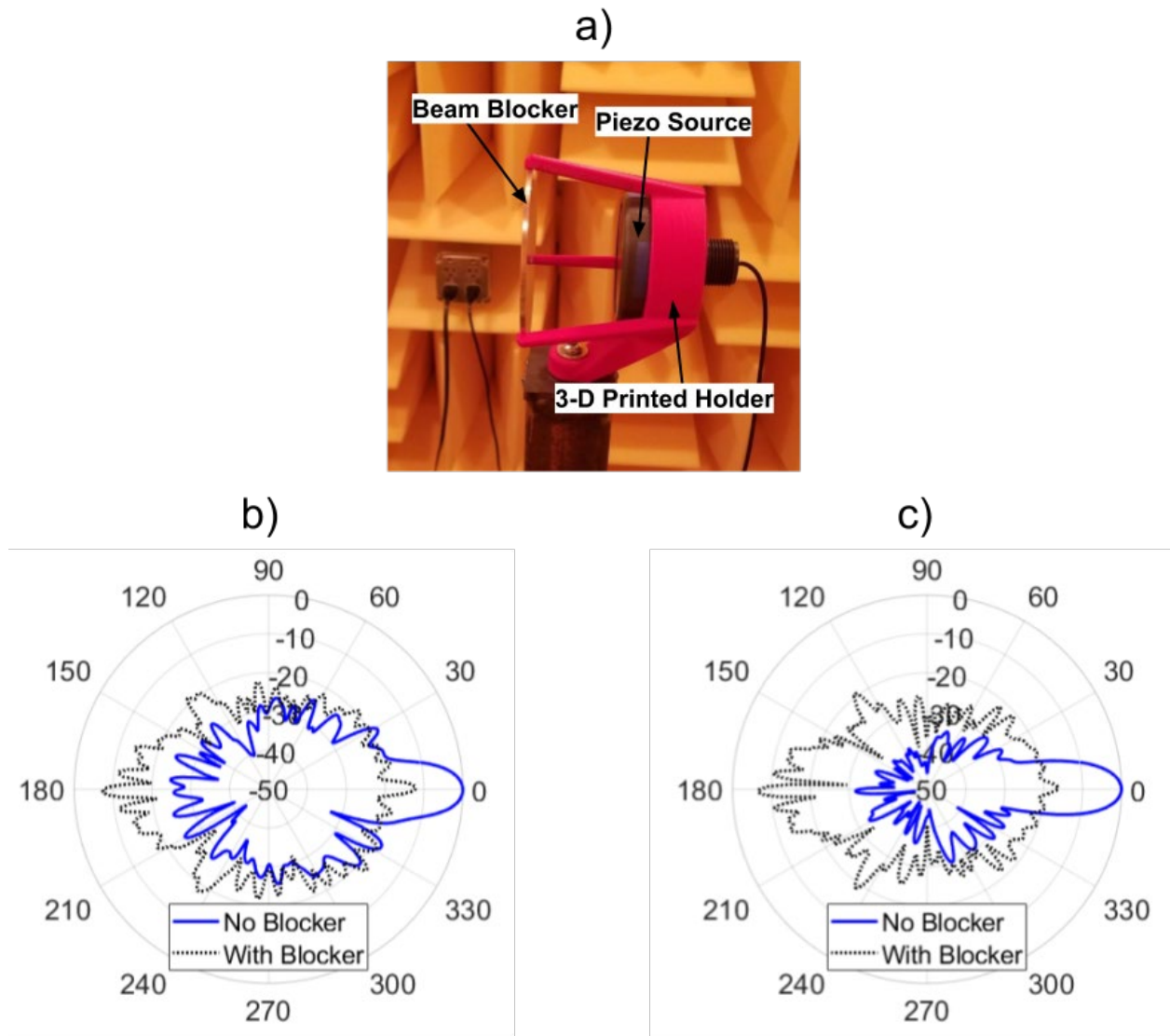


Fig. 3. Photograph and beam patterns of the ultrasonic source. a) Photograph of the source inside the 3D-printed holder, with a beam blocker. b) and c) Beam patterns with and without blockers (dB relative to the no blocker case at 0°) for b) 35.1 kHz - 37.1 kHz bandwidth and c) 38.5 kHz - 40.5 kHz bandwidth, respectively.

The directivity measurements in the horizontal plane were also performed in the same small anechoic chamber as the absorption coefficient measurement was made in. An Outline ET250-3D Turntable was used to make measurements every 1° . A metal stand was fabricated to mount the 3D-printed holders to the turntable (about 1 m tall). At each angle, a 35-46 kHz chirp was

broadcast from the source, and recorded with the 6.35 mm microphone. A sampling frequency of 5 MHz was used. The excitation signal contained a 500 ms long chirp signal. The spectrum at each angle was calculated, and at each frequency within the 2 kHz-wide bandwidths of interest, the amplitudes were squared and summed. This dB value was referenced to the maximum value of the no blocker case for the given bandwidth. Both the blocker and no blocker case (for a given frequency bandwidth) thus have the same reference.

2.5 Transducer Response

The average, measured, electrical impedance of the 8 sources used is shown in Fig. 4 (a). At 45 kHz, the impedance dips to 80 Ω . This was problematic, because the transducers draw too much current from the amplifiers. The Tegam 2350 amplifiers that were used had an output current limit of 40 mA. With the transducer at 80 Ω , this only allowed them to go up to 3.2 V from the amplifier into the source before reaching the current limit. It was decided to avoid this piezoelectric resonance by staying below 41 kHz. Impedance measurements were taken using a Zurich Instruments MFIA Impedance Analyzer.

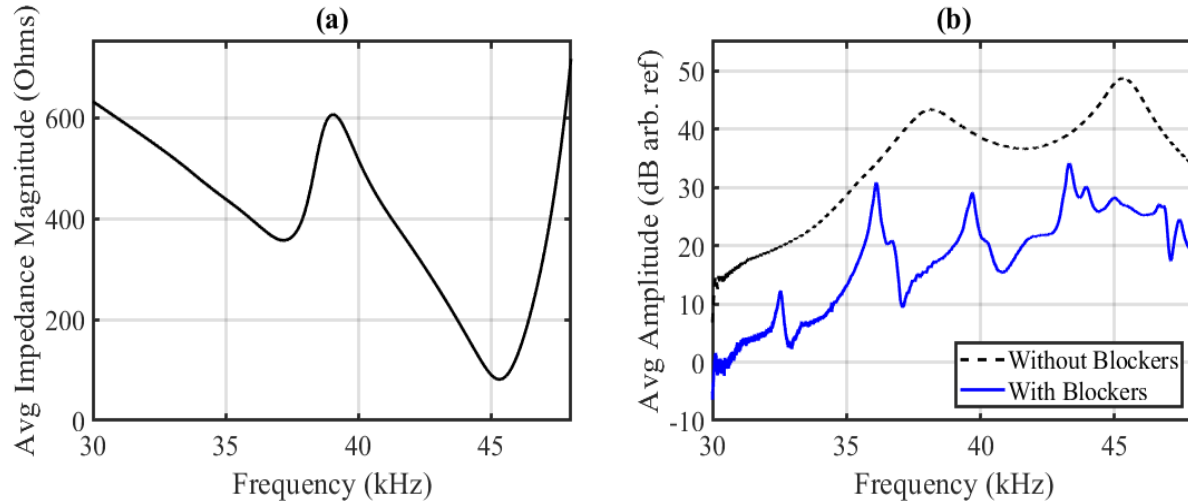


Fig. 4 (a) Average electrical impedance of 8 piezoelectric sources. (b) Average acoustic frequency response of 8 piezoelectric sources at 0° relative to microphone.

The impedance still dips to approximately 300Ω at 37 kHz. To correct this problem, 8 transformers were made (one for each source). These transformers had a 4:1 winding ratio (P Core T-38 22x13 Ferrite 192 x 48 #30AWG), which increased the voltage allowed at the output of the amplifier, while keeping the amplifier's output current at or below 40 mA. This increased the total power output from the amps, allowing more power to be transferred to the piezoelectric source.

With the transformers in place, we were able to achieve an output voltage of 150 V from the amplifiers. Because these transformers had a very low (approximately 2.4Ω) impedance for DC signals, a small offset of even 100 mV at the output of the amplifier would draw more than the amplifier's current limit of 40 mA. A $100 \mu\text{F}$ capacitor (that can handle up to 300 VAC) was put in series with the transformer, between the amplifier and transformer, to block DC current. A diagram of the setup is shown in Fig. 5.

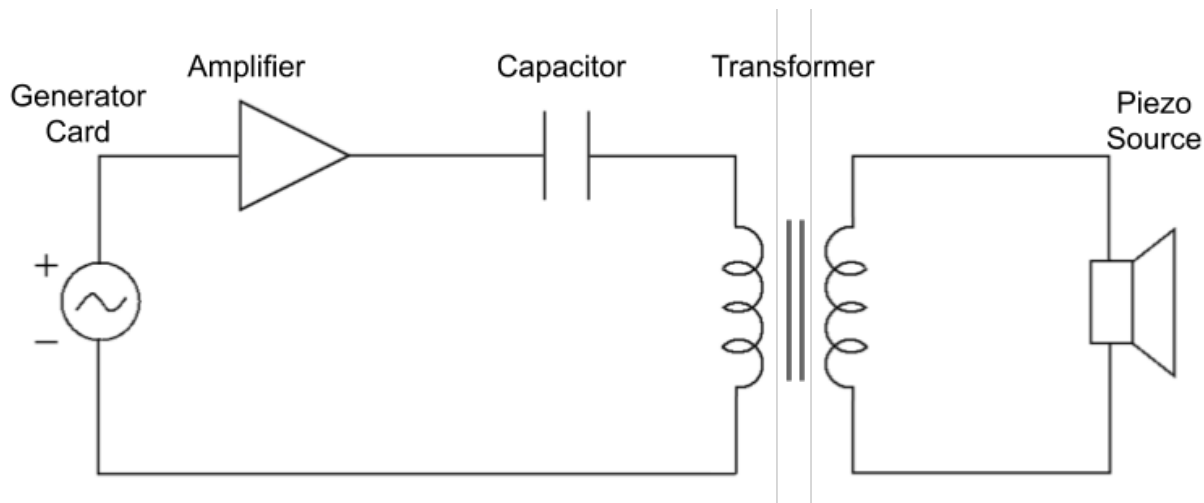


Fig. 5. Setup diagram using generator card, amplifier (triangle), DC blocking capacitor, 4:1 transformer, and source.

Observation of the acoustic frequency response of the piezoelectric sources (Fig. 4b) reveals that the beam blocker introduces its own acoustic resonances. (The beam blockers do not affect the electrical impedance of the sources.) The beam blocker is 4.8 cm away from the face of the source, and creates the expected half-wavelength-multiples modes between the two rigid boundaries (in the axial direction of the source). We chose to center our TR forward bandwidths on two of these new resonances (the 10th and 11th ones), in order to achieve the highest TR amplitudes possible. These two center frequencies were 36.1 kHz and 39.5 kHz.

While using 4 of the sources centered at 36.1 kHz, and the other 4 sources centered at 39.5 kHz, the bandwidth of the forward chirp was changed from 0 to 6 kHz. A TR experiment was performed using clipping with a ratio of 0.01. The sources were used with blockers in place, and sources were pointed roughly 180° (away) from the microphone(s). A 0.3 s chirp was used for the forward step. For both the forward step, 10 averages were taken, and for the backwards step, 50 averages were taken to reduce noise. A peak voltage of 3 V was sent from the generator cards, amplified times 50 before reaching the sources. A sampling frequency of 500 kHz was used. The results are shown in Fig. 6(a).

Since the difference frequency between the two sets of sources is of interest, the bandwidth from each set should be kept below 3.4 kHz, even though wider bandwidths produce higher focal amplitudes. This avoids using bandwidths that overlap for the 2 sets of sources, ($39.5 \text{ kHz} - 36.1 \text{ kHz} = 3.4 \text{ kHz}$, which means 1.7 kHz on each side of the center frequency before they overlap). Since a difference frequency bandwidth centered on 3.4 kHz is expected, the bandwidth from a given source should be lower than 3.4 kHz. Otherwise, the difference frequency may be generated due to nonlinearities from self interactions within an individual source's bandwidth, instead of being generated at the TR focus. A narrow bandwidth is also advantageous because it should create a more clearly defined difference frequency in a frequency spectrum. Therefore, a balance should be found between the larger amplitudes offered by a large bandwidth, and the clarity offered by a narrow bandwidth. The energy in the difference frequency band from 3 kHz – 6.4 kHz was plotted against the bandwidth used for the forward step in Fig. 6(b). In a similar way, the maximum value within the difference frequency band from 3 kHz – 6.4 kHz was plotted against the bandwidth used for the forward step in Fig. 6(c). From these figures, a 500 Hz bandwidth was chosen for generating a difference frequency.

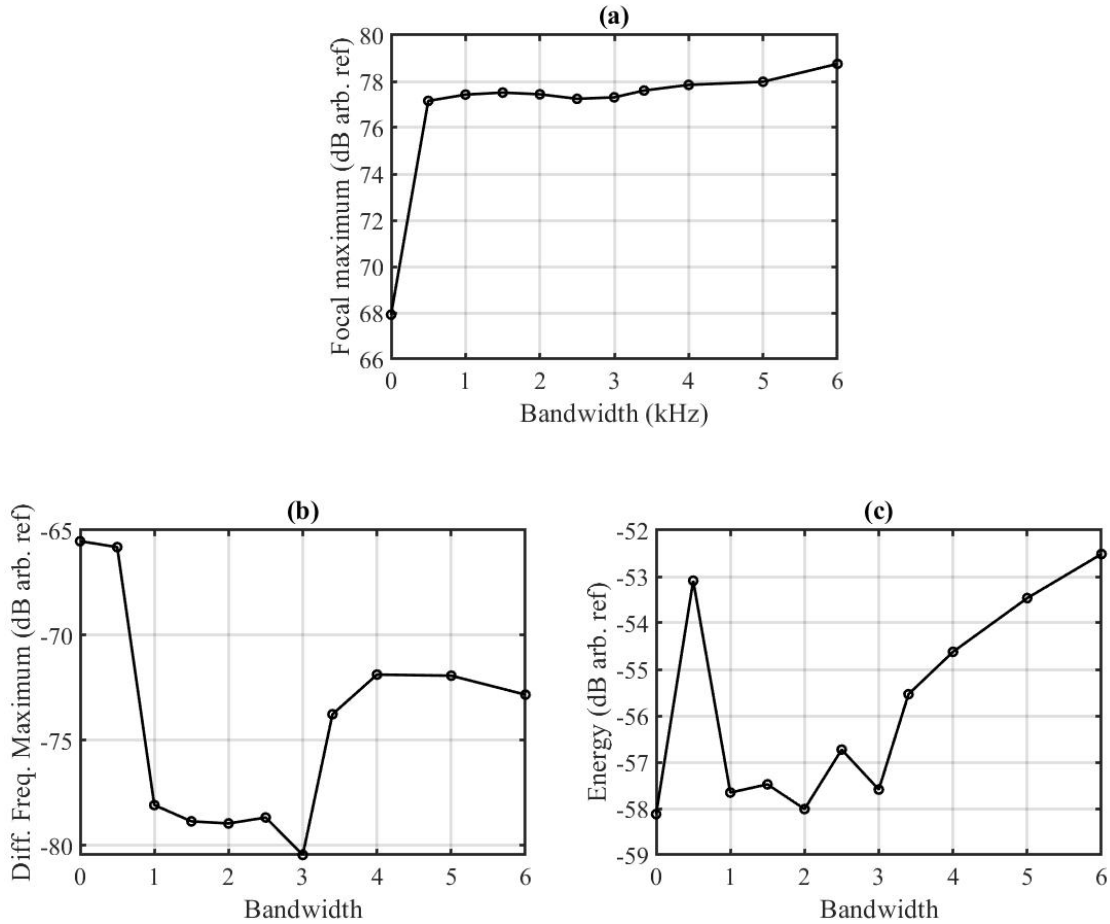


Fig. 6. a) Peak focal amplitude versus forward-step bandwidth with 4 sources centered on 36.1 kHz and 4 sources centered on 39.5 kHz. b) Maximum in difference frequency band vs. forward-step bandwidth. c) Energy in difference frequency band vs. forward-step bandwidth.

It is possible to record a difference frequency of two primary frequencies, even if the parametric array effect is not present. This can be due to microphone distortion.^{24, 34, 49, 50} Several researchers have distinguished between microphone nonlinearities and in-air demodulation by measuring the propagation curve of the on-axis difference frequency signal while varying the distance of the microphone from a parametric array loudspeaker (PAL). If the propagation curve does not follow the theory for a parametric array, this can be a sign of microphone distortion.^{34, 49}

In order to compare the two microphones' responses in detecting a difference frequency, the difference frequency of a PAL (HSS H450 Directed Audio Sound System) was measured at various distances from the PAL. The two microphones were placed end-to-end, such that the grid caps of the microphones were touching (see Fig. 7(a)). They were then moved incrementally away from the PAL as a 1 kHz signal was sent to the PAL (the PAL does the signal processing required to create this 1 kHz difference frequency using ultrasonic primary frequencies). At each microphone position, the voltage sent to the PAL was varied. The signals from each microphone could then be compared each other, and if the pressure amplitudes were different for each microphone, it was an indication of the presence of microphone distortion in at least one of the microphones. To insure that the microphones were calibrated correctly, they were used to measure a 1 kHz signal broadcast from an ordinary loudspeaker. While in their end-to-end configuration, the microphone calibrations, which had been previously measured, gave the same sound pressure levels for each microphone. Thus, the end-to-end configuration did not affect the microphones' ability to record a frequency of 1 kHz. When the PAL was used, it produced a few primary frequencies, including 42 kHz, 43 kHz, and 41 kHz. These high-amplitude primary frequencies produce a difference frequency of 1 kHz (in addition to a weaker 2 kHz signal). A 5 second chirp with a sampling frequency of 5 MHz was used. The comparison of the results at various measurement differences to the expected theory for a parametric array was inconclusive, meaning that some amount of microphone distortion could be an issue for one or both of the microphones.

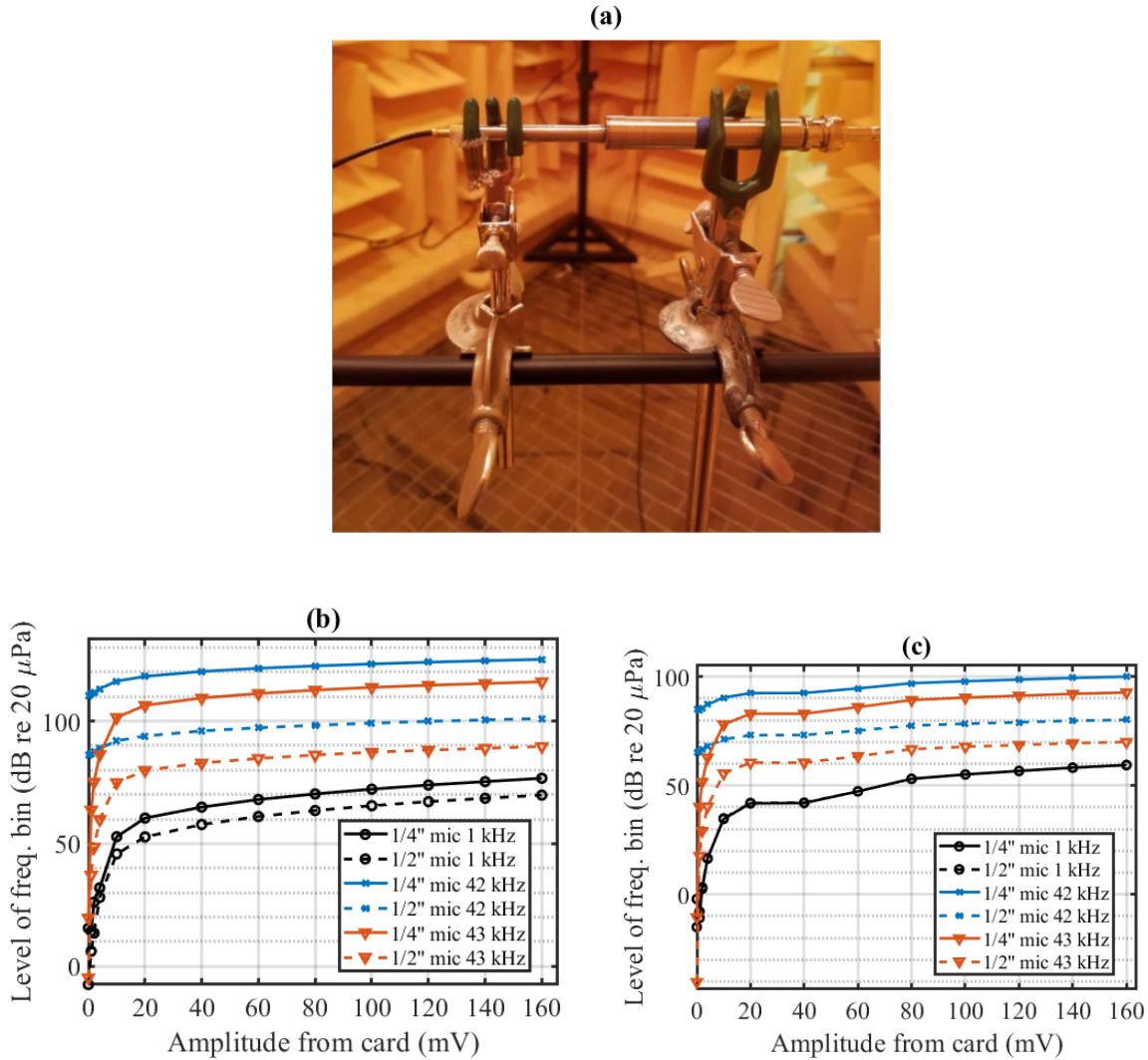


Fig. 7. (a) Configuration of 2 microphones end-to-end, with gridcaps touching. (b) Amplitudes recorded by 2 microphones, 28 cm away from a PAL. Input voltage from the generator card to the PAL is varied. (c) Amplitudes recorded by 2 microphones, 211.5 cm away from PAL. Input voltage from generator card to PAL is varied. 1 kHz signals from both mics lie almost exactly in the same place.

At a distance of 28 cm from the PAL (Fig. 7(b)), the 1 kHz difference frequency amplitudes differ between the two mics, indicating microphone distortion in at least one microphone. At a distance of 211.5 cm from the PAL (Fig. 7(c)), the 1 kHz difference frequency signals lie almost exactly in the same place, indicating little microphone distortion for this distance. Because the 1

kHz difference frequency amplitude is higher in the 6.35 mm microphone than in the 12.7 mm microphone when the microphones are close to the PAL, it is concluded that the 6.35 mm microphone introduces more internal, microphone distortion than the 12.7 mm microphone. This is likely because the 12.7 mm microphone is much less sensitive at 40 kHz, where the primaries are located, so there is less movement of the microphone diaphragm at these frequencies, and less opportunity for distortion to be introduced.

2.6 Time-Varying Impulse Responses

Often in audible-frequency TR experiments, the impulse response remains fairly constant throughout the course of several experiments, and the impulse response can be used for many backwards steps, without needing to re-calculate the impulse response. However, it was found that for this setup with ultrasound in air, the amplitude and time of focus shifted as time passed, if an old impulse response was used. For one such trial, the impulse response was found, and then the backward step was performed repeatedly throughout the course of 43 minutes.

Throughout this time, the peak pressure at the focus decreased with each subsequent recording and arrived earlier in time. After the 43 minutes, the peak pressure amplitude had shifted down by 10.9 % and the focus peak arrived 2.2 μ s earlier than the focus peak measured at time zero.

When the impulse response was re-measured before each backward step, the focal amplitude and arrival times were very consistent between measurements. For these trials, a sampling frequency of 5 MHz was used to capture the narrow focus peak with high resolution. A clipping threshold of 0.01, 10 averages, 2 kHz bandwidth (centered on 35.091 kHz for 4 sources, 39.5 kHz for the other 4 sources), and a 0.5 s chirp were used.

These two effects (lowering amplitude focus and shifting earlier in time) are likely due to small increases in temperature inside the box as time went on. Since sound speed increases as the square root of temperature, an increase in temperature would explain the slightly earlier arrival of the focus. And since the time it takes to traverse the various path lengths changes less for shorter paths than it does for longer paths, the various arrivals of the TRIR no longer arrive at the focus at exactly the same time as each other, and the amplitude of the focus is lowered. The temperature in the room in which the wooden chamber is located is known to typically increase by about 2° C from the morning until the afternoon. This presents a weakness of ultrasonic TR in a room: the impulse response can be affected by small changes in air temperature. This is similar to the findings of Griffa *et al.* and Scalerandi *et al.*^{51, 52}

Chapter 3 Results

3.1 Effect of Directivity on TR Focal Amplitudes

It has been shown by Anderson *et al.* that for somewhat directional sources in reverberant environments, the highest TR focal amplitude is achieved when the sources are pointed away from the microphone.⁵ However, for highly directional sources such as those used here, this is not the case as was alluded to previously.

In order to determine the effect of source directivity on TR focal amplitudes, 8 sources were used to create a TR focus. The peak focal amplitude was recorded for 8 different angles of each source relative to the microphone focus location (0° means that all 8 sources were pointed at the microphone, and the 8 different angles are spaced every 45°). The results are shown in Fig. 8. A

clipping ratio of 0.05 was used. Because Anderson *et al.* did not use clipping in their study,⁵ the results reported in this thesis are not directly comparable to their results. 800 mV were output directly from card to the piezoelectric sources (no amplifier was used). A sampling frequency of 500 kHz was used and the chirp was 100 ms long. The signals were bandpass filtered in the software with a passband of 5 kHz to 150 kHz to reduce noise in the signal. 10 averages were taken.

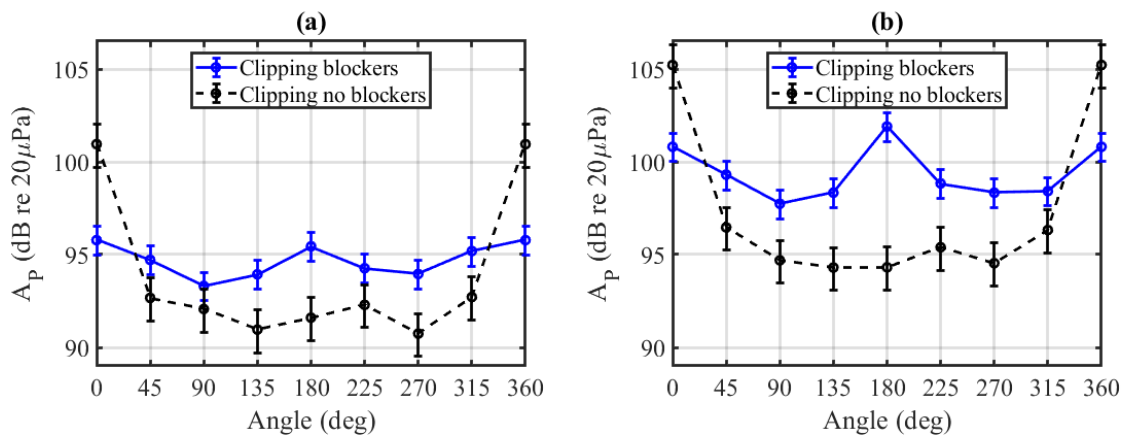


Fig. 8. Time reversal peak focal amplitude for various angles of eight sources with respect to the microphone with and without blockers in place. Forward step chirp bandwidths are (a) 35.1 – 37.1 kHz and (b) 38.5 – 40.5 kHz.

Error bars for Fig. 8 was estimated in the following way. 10 trials were performed (10 averages/trial), changing the position of the sources within the box for each new trial. Whenever the position of the sources was changed, the sources were kept approximately 50 cm or farther from the microphone, and approximately 10 cm or farther from the walls. For all trials, the sources were pointed directly toward the microphone (0°). The forward chirp were centered on 36.1 kHz, each with a bandwidth of 2 kHz. The error for the 0° position with a bandwidth centered on 36.1 kHz is assumed to be representative of the error for all other angles, as well as

for the bandwidth centered on 39.5 kHz. The error found for this angle and bandwidth is applied to all other measurements. For these 10 trials, the experiment was performed both with the blockers in place, and with no blockers. With the blockers in place, the mean focal amplitude between the 10 trials was 1.30 Pa, with a range of 0.40 Pa (min: 1.17 Pa; max: 1.57 Pa), and a standard deviation of 0.115 (relative standard deviation: 0.0886). With no blockers in place, the mean focal amplitude between the 10 trials was 2.12 Pa, with a range of 1.01 Pa (min: 1.75 Pa; max: 2.76 Pa), and a standard deviation of 0.281 Pa (relative standard deviation: 0.132). The error bounds on the figure were calculated by moving one standard deviation away from the measured focal amplitude value at each angle.

The highest-amplitude focus is generated when the sources are used with no blockers, and are pointed directly at the microphone. However, when the sources are not pointed at the microphone, the highest-amplitude focus is usually created when the sources are used with beam blockers. Thus beam blockers provide an advantage for creating a focus at any selected location within the room for which the location would be at an arbitrary direction relative to the sources.

3.2 Peak Levels Achieved at Focus

Because the peak focal amplitude is often reported in this thesis, we use the symbol A_P to denote peak focal amplitude. Whenever this value is reported as a decibel value, it refers to the peak decibel value (not the RMS value). In order to generate as high an A_P as possible, all 8 sources were used in a TR experiment. We found that a bandwidth covering both resonances of the piezoelectric source-blocker setup yielded a higher A_P , therefore a bandwidth from 35.1 kHz – 40.5 kHz was used. A sampling frequency of 5 MHz was used to improve the resolution of the

narrow focal peak. A forward chirp of 300 ms and clipping with a threshold of 0.01 were used. The generator cards were used at their maximum voltage of $\pm 3 V_{\text{peak}}$ (which was then amplified). 10 averages were taken. A_p for this measurement was 134 dB re 20 μPa .

3.3 Nonlinear Difference Frequency Generation

In order to generate a difference frequency at a TR focus, 4 sources were centered on 36.1 kHz, and 4 sources were centered on 39.5 kHz. A bandwidth of 500 Hz was used. 50 averages were used on the backward step to decrease noise in the spectrum. A 300 ms chirp with a clipping threshold of 0.01 and sampling frequency of 500 kHz was used. Recordings from the 12.7 mm microphone were analyzed, because this microphone likely introduces less microphone distortion than the 6.35 mm microphone.

In order to determine if the difference frequency content increased nonlinearly in response to a linear change in voltage sent to the piezoelectric sources, varying voltages were sent from the generator cards, and the results were scaled such that if the TR focusing was a linear process, the plotted amplitudes would be the same for the focuses of the highest- and lowest-amplitude voltage signals sent from the generator cards.¹³ The spectra for 4 of these voltages were then plotted (Fig. 9(a)) for these linearly scaled data, and compared (Fig. 9(b)). The unscaled energies within the bandwidth from 3 kHz – 4 kHz are plotted against the unscaled energies in the primary frequencies (35 kHz – 40 kHz). Figure 9(c) shows energy (arb. ref.) of the primaries from 35 kHz - 40 kHz vs. energy (different arb. ref.) of the difference frequency band from 3 kHz – 4 kHz. Figure 9(d) shows the maximum unscaled amplitude within the aforementioned primary band vs. the maximum unscaled amplitude in the difference frequency band. The very

presence of difference frequency content indicates nonlinearity somewhere in the system. On close inspection of the difference frequency spectra, there appears to be some amount of nonlinear scaling. In Fig. 9(c) and Fig. 9(d) it becomes clear that the difference frequency content increases nonlinearly with increasing primary frequency content.

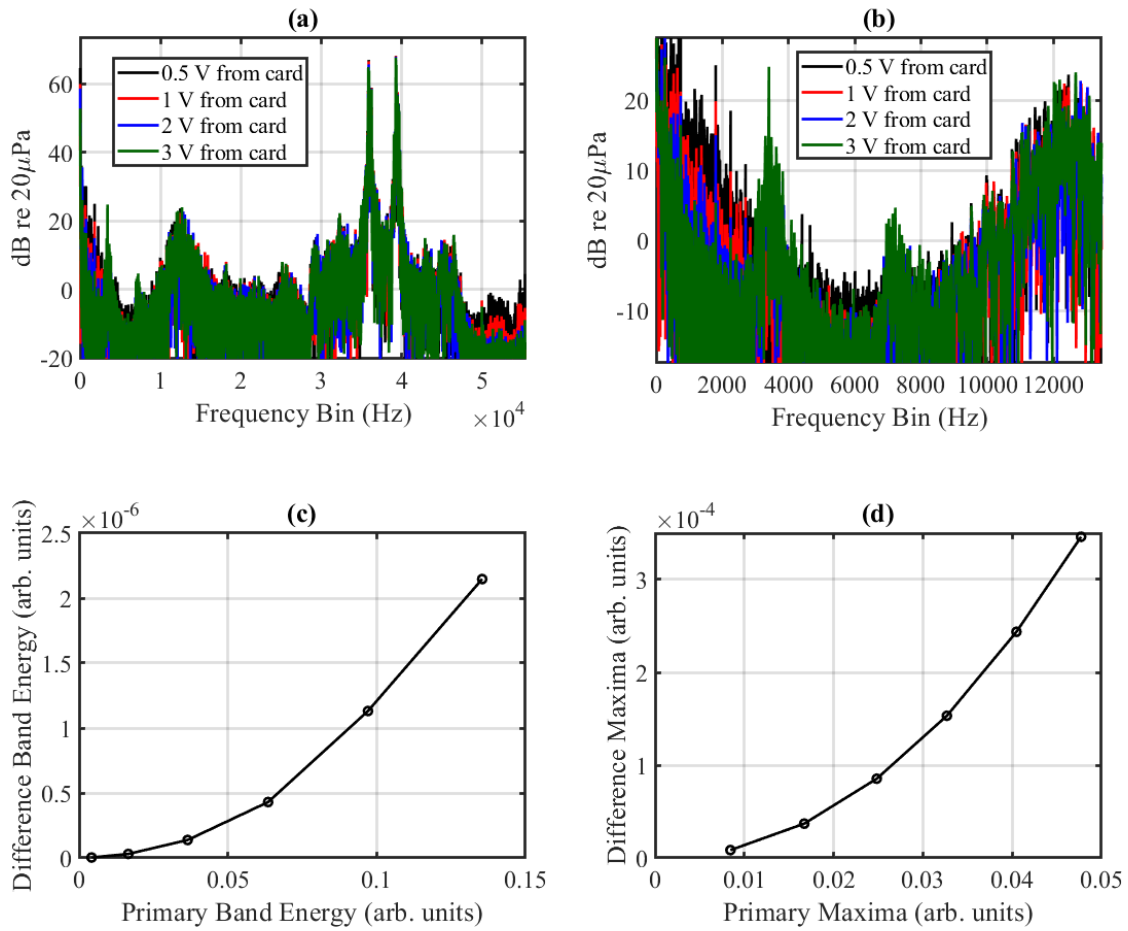


Fig. 9 (a) Scaled spectra of focus signal. (b) Scaled focus signal spectra zoomed in on difference frequency content. (c) Difference frequency energy (3-4 kHz) vs. primary frequency energy (35-40 kHz). (d) Maximum within difference frequency band vs. maximum within primary band.

Chapter 4 Conclusions

When using a highly directional source in a reverberant environment, the highest TR focal amplitude is achieved when the sources are pointed directly at the focal location. However, the use of a beam blocker to make the sources more omnidirectional increases the focal amplitude for every other angle of the sources relative to the focal location. Thus the precise alignment of the sources with respect to any desired focal location is not necessary with the use of beam blockers. The use of a more omnidirectional source may also increase the ability to create a “virtual sound source” at the focus of a TR process.

Evidence of nonlinearity at the focus of a high-amplitude ultrasonic TR process was seen. When using 4 sources at one frequency bandwidth, and another 4 sources at a different bandwidth, a difference frequency at the microphone was recorded. The degree to which this difference frequency is due to internal intermodulation distortion in the microphone, due to

noncollinear interaction of sound with sound, or due to nonlinear parametric array type effects is yet to be determined.

References

- [1] M. Fink, "Time Reversed Acoustics," *Phys. Today* **50**, 34-40 (1997).
- [2] B. E. Anderson, M. Griffa, C. Larmat, T. J. Ulrich, and P. A. Johnson, "Time Reversal," *Acoust. Today* **4**(1), 5-16 (2008).
- [3] C. Draeger, J-C. Aime, and M. Fink, "One-channel time reversal in chaotic cavities: Experimental results," *J. Acoust. Soc. Am.* **105**(2), 618-625 (1999).
- [4] B. Van Damme, K. Van Den Abeele, Y. Li, and O. Bou Matar, "Time reversed acoustics techniques for elastic imaging in reverberant and nonreverberant media: An experimental study of the chaotic cavity transducer concept," *J. Appl. Phys.* **109**(10), 104910 (2011).
- [5] B. E. Anderson, M. Clemens, and M. L. Willardson, "The effect of transducer directivity on time reversal focusing," *J. Acoust. Soc. Am.* **142**(1), EL95-EL101 (2017).
- [6] A. Parvulescu and C. S. Clay, "Reproducibility of signal transmissions in the ocean," *Radio Elec. Eng.* **29**(4), 223-228 (1965).
- [7] C. S. Clay and B. Anderson, "Matched signals: The beginnings of time reversal," *Proc. Mtgs. Acoust.* **12**(1), 055001 (2011).
- [8] J. V. Candy, A. J. Poggio, D. H. Chambers, B. L. Guidry, C. L. Robbins, and C. A. Kent, "Multichannel time-reversal processing for acoustic communications in a highly reverberant environment," *J. Acoust. Soc. Am.* **118**(4), 2339-2354 (2005).
- [9] J. V. Candy, A. W. Meyer, A. J. Poggio, and B. L. Guidry, "Time-reversal processing for an acoustic communications experiment in a highly reverberant environment," *J. Acoust. Soc. Am.* **115**(4), 1621-1631 (2004).
- [10] A. W. Meyer, J. V. Candy, and A. J. Poggio, "Time reversal signal processing in communications—A feasibility study," *Lawrence Livermore National Laboratory Library*, (2002).
- [11] G. Ribay, J. de Rosny, and M. Fink, "Time reversal of noise sources in a reverberation room," *J. Acoust. Soc. Am.* **117**(5), 2866-2872 (2005).
- [12] M. H. Denison and B. E. Anderson, "Time reversal acoustics applied to rooms of various reverberation times," *J. Acoust. Soc. Am.* **144**(6), 3055-3066 (2018).
- [13] M. L. Willardson, B. E. Anderson, S. M. Young, M. H. Denison, and B. D. Patchett, "Time reversal focusing of high amplitude sound in a reverberation chamber," *J. Acoust. Soc. Am.* **143**(2), 696-705 (2018).

- [14] C. Prada, E. Kerbrat, D. Cassereau, and M. Fink, "Time reversal techniques in ultrasonic nondestructive testing of scattering media," *Inv. Prob.* **18**(6), 2002).
- [15] B. E. Anderson, L. Pieczonka, M. C. Remillieux, T. J. Ulrich, and P-Y. Le Bas, "Stress corrosion crack depth investigation using the time reversed elastic nonlinearity diagnostic," *J. Acoust. Soc. Am.* **141**(1), EL76-EL81 (2017).
- [16] S. M. Young, B. E. Anderson, S. M. Hogg, P-Y. Le Bas, and M. C. Remillieux, "Nonlinearity from stress corrosion cracking as a function of chloride exposure time using the time reversed elastic nonlinearity diagnostic," *J. Acoust. Soc. Am.* **145**(1), 382-391 (2019).
- [17] B. E. Anderson, M. C. Remillieux, P-Y. Le Bas, and T. J. Ulrich, Time Reversal Techniques, in *Nonlinear Ultrasonic and Vibro-Acoustical Techniques for Nondestructive Evaluation*, edited by Tribikram Kundu, (Springer International Publishing, Cham, 2019), pp. 547-581.
- [18] N. Smagin, A. Trifonov, O. Bou Matar, and V. V. Aleshin, "Local damage detection by nonlinear coda wave interferometry combined with time reversal," *Ultrason.* **108**, 106226 (2020).
- [19] G. Montaldo, P. Roux, A. Derode, C. Negreira, and M. Fink, "Ultrasound shock wave generator with one-bit time reversal in a dispersive medium, application to lithotripsy," *Appl. Phys. Lett.* **80**(5), 897-899 (2002).
- [20] J-L. Thomas, F. Wu, and M. Fink, "Time Reversal Focusing Applied to Lithotripsy," *Ultrason. Imaging* **18**(2), 106-121 (1996).
- [21] J-L. Thomas and M. Fink, "Ultrasonic beam focusing through tissue inhomogeneities with a time reversal mirror: application to transskull therapy," *IEEE Trans. Ultrason. Ferr. Freq. Contr.* **43**(6), 1122-1129 (1996).
- [22] M. Tanter, J-L. Thomas, and M. Fink, "Focusing and steering through absorbing and aberrating layers: Application to ultrasonic propagation through the skull," *J. Acoust. Soc. Am.* **103**(5), 2403-2410 (1998).
- [23] S. M. Young, B. E. Anderson, M. L. Willardson, P. E. Simpson, and P-Y. Le Bas, "A comparison of impulse response modification techniques for time reversal with application to crack detection," *J. Acoust. Soc. Am.* **145**(5), 3195-3207 (2019).
- [24] N. Roy, H. Hassanieh, and R. R. Choudhury, "BackDoor: making microphones hear inaudible sounds," in *Proc. 15th Ann. Int. Conf. Mobile Sys. App. Services*, (ACM, New York, NY, USA, 2017) pp. 2-14.
- [25] Y. Chen, H. Li, S. Teng, S. Nagels, Z. Li, P. Lopes, B. Y. Zhao, and H. Zheng, "Wearable microphone jamming," in *Proc. 2020 CHI Conf. Human Factors Comput. Sys.* (ACM, New York, NY, USA, 2020) pp. 1-12.

- [26] M. Ueda, A. Ota, and H. Takahashi, "Investigation on high-frequency noise in public space," *Inter-noise*, (2014).
- [27] T. G. Leighton, "Ultrasound in air-Guidelines, applications, public exposures, and claims of attacks in Cuba and China," *J. Acoust. Soc. Am.* **144**(4), 2473-2489 (2018).
- [28] M. D. Fletcher, S. L. Jones, P. R. White, C. N. Dolder, T. G. Leighton, and B. Lineton, "Effects of very high-frequency sound and ultrasound on humans. Part I: Adverse symptoms after exposure to audible very-high frequency sound," *J. Acoust. Soc. Am.* **144**(4), 2511-2520 (2018).
- [29] M. D. Fletcher, S. L. Jones, P. R. White, C. N. Dolder, T. G. Leighton, and B. Lineton, "Effects of very high-frequency sound and ultrasound on humans. Part II: A double-blind randomized provocation study of inaudible 20-kHz ultrasound," *J. Acoust. Soc. Am.* **144**(4), 2521-2531 (2018).
- [30] A. van Wieringen and C. Glorieux, "Assessment of short-term exposure to an ultrasonic rodent repellent device," *J. Acoust. Soc. Am.* **144**(4), 2501-2510 (2018).
- [31] M. D. Fletcher, S. Lloyd Jones, P. R. White, C. N. Dolder, B. Lineton, and T. G. Leighton, "Public exposure to ultrasound and very high-frequency sound in air," *J. Acoust. Soc. Am.* **144**(4), 2554-2564 (2018).
- [32] C. Shi, Y. Kajikawa, and W. Gan, "An overview of directivity control methods of the parametric array loudspeaker," *APSIPA Trans. Sig. Info. Proc.* **3**, e20 (2014).
- [33] P. J. Westervelt, "Parametric End-Fire Array," *J. Acoust. Soc. Am.* **32**(7), 934-935 (1960).
- [34] M. B. Bennett and D. T. Blackstock, "Parametric array in air," *J. Acoust. Soc. Am.* **57**(3), 562-568 (1975).
- [35] P. J. Westervelt, "Parametric Acoustic Array," *J. Acoust. Soc. Am.* **35**(4), 535-537 (1963).
- [36] P. J. Westervelt, "Scattering of Sound by Sound," *J. Acoust. Soc. Am.* **29**(8), 934-935 (1957).
- [37] U. Ingard and D. C. Pridmore-Brown, "Scattering of Sound by Sound," *J. Acoust. Soc. Am.* **28**(3), 367-369 (1956).
- [38] J. L. S. Bellin and R. T. Beyer, "Scattering of Sound by Sound," *J. Acoust. Soc. Am.* **32**(3), 339-341 (1960).
- [39] L. W. Dean, "Interactions between Sound Waves," *J. Acoust. Soc. Am.* **34**(8), 1039-1044 (1962).
- [40] J. J. Truchard, "Parametric receiving array and the scattering of sound by sound," *J. Acoust. Soc. Am.* **64**(1), 280-285 (1978).

- [41] J. A. Ten Cate, "Scattering of sound by sound: Nonlinear interaction of collinear and noncollinear sound beams," Ph.D. Thesis Univ. of Texas, Austin, (1992).
- [42] P. J. Westervelt, "Answer to criticism of experiments on the scattering of sound by sound," *J. Acoust. Soc. Am.* **95**(5), 2865 (1994).
- [43] P. J. Westervelt, "Answer to criticism of my treatment of nonscattering of sound by sound," *J. Acoust. Soc. Am.* **95**(5), 2865 (1994).
- [44] P. J. Westervelt, "Scattering of sound by sound within the interaction zone," *J. Acoust. Soc. Am.* **96**(5), 3320 (1994).
- [45] M. F. Hamilton and J. A. TenCate, "Sum and difference frequency generation due to noncollinear wave interaction in a rectangular duct," *J. Acoust. Soc. Am.* **81**(6), 1703-1712 (1987).
- [46] B. E. Anderson, T. J. Ulrich, and P-Y. Le Bas, "Comparison and visualization of focusing wave fields from various time reversal techniques in elastic media," *J. Acoust. Soc. Am.* **134**(6), EL527-EL533 (2013).
- [47] M. H. Denison and B. E. Anderson, "The effects of source placement on time reversal focusing in rooms," *Appl. Acoust.* **156**, 279-288 (2019).
- [48] T. Jenny and B. E. Anderson, "Ultrasonic anechoic chamber qualification: Accounting for atmospheric absorption and transducer directivity," *J. Acoust. Soc. Am.* **130**(2), EL69-EL75 (2011).
- [49] C. Ye, Z. Kuang, M. Wu, and J. Yang, "Development of an Acoustic Filter for Parametric Loudspeaker in Air," *Jap. J. Appl. Phys.* **50**(7), 07HE18 (2011).
- [50] P. Ji and J. Yang, "An experimental investigation about parameters' effects on spurious sound in parametric loudspeaker," *Appl. Acoust.* **148**, 67-74 (2019).
- [51] M. Griffa, B.E. Anderson, R.A. Guyer, T.J. Ulrich, P.A. Johnson, "Investigation of the robustness of time reversal acoustics in solid media through the reconstruction of temporally symmetric sources," *J. Phys. D: Appl. Phys.* **41**(8), 085415 (2008).
- [52] M. Scalerandi, M. Griffa, P.A. Johnson, "Robustness of computational time reversal imaging in media with elastic constant uncertainties," *J. Appl. Phys.* **106**(11), 114911 (2009).